CO_2 adsorption on pristine, oxidized, and diethylamine-functionalized activated carbon sorbents

Vitaly E. Diyuk[1], *Alexander N.* Zaderko[1], *Liudmyla M.* Grischenko[1], *Galyna G.* Tsapyuk[1], *Anna V.* Vakaliuk[1], *Vladyslav V.* Lisnyak[1,2], and *Ruslan* Mariychuk[2,*]

[1]Taras Shevchenko National University of Kyiv, Chemical Faculty, 01601 Kyiv, Ukraine
[2]Prešov University in Prešov, Faculty of Humanities and Natural Sciences, 08001 Prešov, Slovakia

Abstract. Adsorption is currently the most promising capture technology to shorten atmospheric emissions of carbon dioxide (CO_2). In this article, we report on the adsorption of CO_2 onto pristine, oxidized, and aminated activated carbon (AC) sorbents. From our findings, some functionalized AC sorbents have shown very promising results in the CO_2 capture process. Their maximum adsorption capacity measured by the thermogravimetric method at 20 °C varies between 2.2 and 3.9 mmol CO_2/g depending on the content of diethylamino and oxygen-containing groups. The functionalization of the carbon surface with diethylamino groups improves the adsorption capacity by 30–40%. The CO_2 adsorption little depends on the texture parameters of the pristine AC sorbents. In the range from 20 to 100 °C, the CO_2 thermodesorption showed the effective regeneration of the sorbents. The aminated carbon surface demonstrates the best CO_2 adsorption but binds the adsorbed molecules stronger than the oxidized surface, which limits the sorbent regeneration.

1 Introduction

Energy consumption and economic growth are known reasons for atmospheric pollution [1, 2], so capturing greenhouse gases becomes an actual task [3]. Adsorption is the most promising technology to shorten emissions of carbon dioxide (CO_2) [4]. Activated carbon (AC) sorbents are reasonable materials for such a purpose. Their large specific surface area and developed porosity can support effective CO_2 adsorption [5, 6]. In addition, one can graft CO_2-capturing organic groups on the carbon surface [7-9].

In this work, we will focus on the adsorption of CO_2 on pristine, oxidized, and aminated AC sorbents. The impact of the surface functionalization with oxygen- and nitrogen-containing groups will be considered. We will compare the adsorptive capacity of CO_2 at elevated temperatures and will present correlations between CO_2 adsorption parameters for studied sorbents.

* Corresponding author: ruslan.mariychuk@unipo.sk

2 Experimental

In this work, we used several AC sorbents, having developed microporous structure, namely, granulated AC produced from biomass (ACB), spherical, granulated, nitrogen-containing AC (SCN), and AC hemosorbent (HSGD). Three series of functionalized AC sorbents were prepared by oxidation, halogenation followed amination, and direct amination.

Oxidation. 2 g of selected AC sorbent was added to a 20% (v/v) solution of HNO_3 (60 ml) and refluxed on a sand bath at 80 °C for 2 h. The oxidized AC sorbents (ACBox, SCNox, and HSGDox) were washed from acid residues to pH 5.5–6.0 by decantation with double-distilled water (DDW). Finally, they were dried in a drying oven at 120 °C for a day.

Bromination. 1 g of selected AC sorbent was wet treated with a mixture of 10% (w/v) Br_2 and 15% (w/v) KBr aqueous solutions, marked future as KBr_3. In a typical bromination, a pre-dried AC sorbent (5 g) was immersed in 50 ml of KBr_3 solution and was left at room temperature for 1 h. The low-bonded and physisorbed bromine were fixed with an aqueous solution of 10% (w/w) $K_2C_2O_4$ (200 ml) [10]. This solution was added in small portions under stirring. When the release of CO_2 gas was ceased, the resulting ACB-Br, SCN-Br, and HSGD-Br samples were filtered and washed extensively from bromide ions with DDW, and then all samples were dried in air at 120 °C.

Gas-phase chlorination. The selected AC sorbent was treated at 450 °C with CCl_4 vapors diluted by argon gas. The treatment was carried out at a flow rate of 40 ml/min for 2 h. By saturation of the argon stream with a CCl_4 vapor at 20 °C, we set the CCl_4 concentration in the argon flow to 1.2 mmol/l. The resulting ACB-Cl, SCN-Cl, and HSGD-Cl samples were vacuumed for 2 h to remove adsorbed gases.

Amination. The halogenated AC sorbents were aminated in a diethylamine alcoholic solution that holds in an autoclave at 120 °C. This is the simplest way that doesn't require surfactants and can be used instead of wet impregnation [10, 11]. The prepared aminated AC sorbents were thoroughly washed and dried in air at 120 °C. Also, the pristine AC sorbents were aminated with a diethylamine vapor at 200–250 °C. After amination, the prepared samples were vacuumed to remove adsorbed species and dried in air at 120 °C. The resulting aminated AC sorbents were marked consistent with the treatment sequence, as AC-Hal-N and AC-N, where AC = ACB, SCN, and HSGD.

Measurements of CO_2 adsorption-desorption were carried out by passing a flow of pure CO_2 gas from a gas bottle (25 ml/min) through a sample (~50 mg) up to the constant sample weight. The maximum adsorption capacity of CO_2 (a_m) was found from the adsorption curves registered at 20 °C. Times required for 50% and 90% CO_2 adsorption ($\tau(50\%)$) and $\tau(90\%)$) with respect to a_m were estimated similarly. CO_2-saturated sorbents were heated in a stream of CO_2 from 20 to 100 °C [12]. Quasi-equilibrium conditions between the adsorbed and gas-phase CO_2 were set by a heating rate of 1 °C/min. CO_2 adsorption at 50 °C and 100 °C (a(50 °C) and a(100 °C)), which was measured from these experiments, is an important parameter when one considers the capturing of hot greenhouse gases. The magnitude a(100 °C) quantifies the regeneration ability of sorbents that depends on the strength of CO_2 adsorption.

Fourier transformed infrared (FTIR) spectra in the attenuation total reflection (ATR) mode were recorded on a Shimadzu IRPrestige 21 spectrophotometer equipped with a Pike ATR accessory with a ZnSe crystal. Scanning electron microscopy (SEM) micrographs providing topographical information were collected on a Zeiss EVO 50 scanning electron microscope. Specific surface areas (S_{BET}) and pore volume (V_S) were determined by nitrogen adsorption measured on a Quantachrome Autosorb-1 gas porosimeter. Thermogravimetry (TG) and derivative thermogravimetry (DTG) analysis were carried out

in argon [13, 14]. Concentrations of O-containing and amino groups (C_{fg}) were found from the TG data. Thermal programmed desorption mass spectroscopy (TPD MS) was performed on a monopole mass spectrometer MX 7304A [15].

3 Results and Discussion

Table 1 sums up the composition and texture parameters of the pristine sorbents. SEM micrographs show that their surface morphology is different (Fig. 1).

Table 1. Composition and texture parameters.

Sorbent	Elemental analysis				Texture parameters	
	C	O	N	Cl	S_{BET}, m²/g	V_S, cm³/g
ACB	95.8	4.1	-	0.1	1,350	0.45
SKN	96.8	2.8	2.4	-	1,300	1.09
HSGD	97.7	2.3	-	-	2,500	3.06

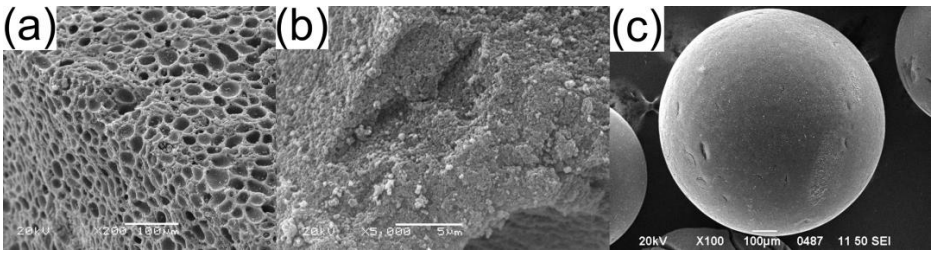

Fig. 1. SEM micrographs of (**a**) ACB, (**b**) SCN, and (**c**) HSGD.

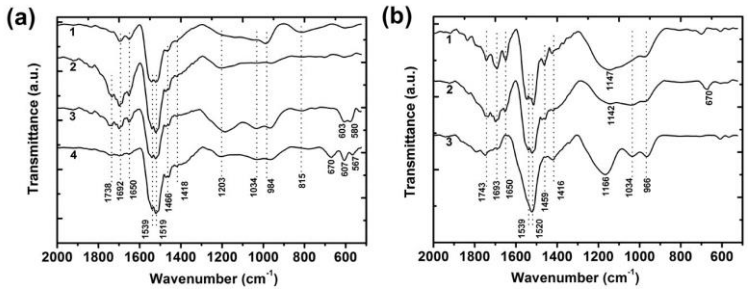

Fig. 2. FTIR spectra of AC sorbents. (**a**) SCN (**1**), SCNox (**2**), SCN-Br (**3**), and SCN-Cl (**4**); (**b**) SCN-Br-N (**1**), SCN-Cl-N (**2**), and SCN-N (**3**).

Surface chemistry changes will be demonstrated on the example of the SCN-based AC sorbents. Figure 2 shows the spectral variations that are caused the surface functionalization. Here, we assign the spectral bands according to infrared characteristic group frequencies reported in [16, 17]. All spectra have the most intensive bands at 1,539 and 1,519 cm^{-1} from skeletal vibrations of aromatic C=C bonds in the carbon matrix. Absorption bands of low intensity at 1,692 and 1,650 cm^{-1} correspond to ν(C=O) in the carbonyl (Cb) groups. The absorption band at 1,203 cm^{-1} and shoulder at 1,418 cm^{-1} are sourced from the ν(C–OH) and ν(O–H) of phenolic (Ph) groups, respectively. Bands at 984 and 1034 cm^{-1} correspond to ν(C–O–C) in ester (E) and anhydride/lactone (A/L) groups, correspondingly. The SCN sample has a slightly oxidized surface (Fig. 2a, spectrum (**1**)). The spectrum of the oxidized SCN shows the increased intensity of bands at 1,750–1,640 cm^{-1} (carboxyl (Cx) groups) and 1,220–960 cm^{-1} (Ph groups) wavelength ranges (see Fig.

2a, spectrum (**2**)). Bromination causes a significant increase in the intensity of the absorption bands at 1,203 and 1,034 cm^{-1} (Fig. 2a, spectrum (**3**)). This increase corresponds to the surface oxidation forming Ph and (C–O–C) groups [18]. Characteristic bands of Cx groups have a similar intensity in the spectra of the SCN-Br and SCN samples. This suggests the formation of Ph, instead of Cx, A, and L groups, at bromination. In the spectrum of SCN-Br, we register low-intensive *ν*(C–Br) bands at 603 and 580 cm^{-1}. In the spectrum of SCN-Cl, the absorption bands in the region 1,750–1,640 cm^{-1} are practically disappearing because of the thermal decomposition of Cx, A, and L groups at chlorination at 450 °C. However, absorption bands at 1,203 and 1,418 cm^{-1} (Ph groups) and at 1,034 and 984 cm^{-1} (E groups) have remained since the temperature of 450 °C is below their thermal decomposition range. In the spectrum of SCN-Cl, we assign the bands of low intensity at 670, 607, and 567 cm^{-1} to vibrations of Cl-containing groups, e.g., C–Cl, $–CCl_3$, etc. The most intensive absorption bands in the spectra of the aminated SCNs (Fig. 2b, spectra (**1-3**)) have the same intensity as in the spectra of SCN and SCNox. In the spectra of SCN-N, SCN-Br-N, and SCN-Cl-N, we registered new vibration bands peaked at 1,166, 1,147, and 1,142 cm^{-1}. We attribute them to stretching vibrations of C–N in the amino groups. The vibration band at 1,166 cm^{-1} is the most intensive in the spectrum of the SCN-N sample. However, the Ph and E groups, which absorb within the same, specific frequency range, can impact on the bandwidth and can shift the peak position. As can be seen from the spectrum of SCN-Br-N, the stretching vibration bands at 603 and 580 cm^{-1} are disappeared. This supports our assumption about the complete removal of bromine from the carbon surface at the amination. But in the spectrum of SCN-Cl-N, the band at 670 cm^{-1} show only a slight decrease in the intensity because of the partial removal of chlorine at amination. FTIR spectra of the oxidized and aminated AC sorbents showed a significant amount of all types of O-containing groups. These groups are products of the parallel oxidation of carbon surface and hydrolysis of the most reactive halogen-containing groups [19, 20]. Figure 2b confirms the presence of diethylamine groups for all the aminated SCN samples.

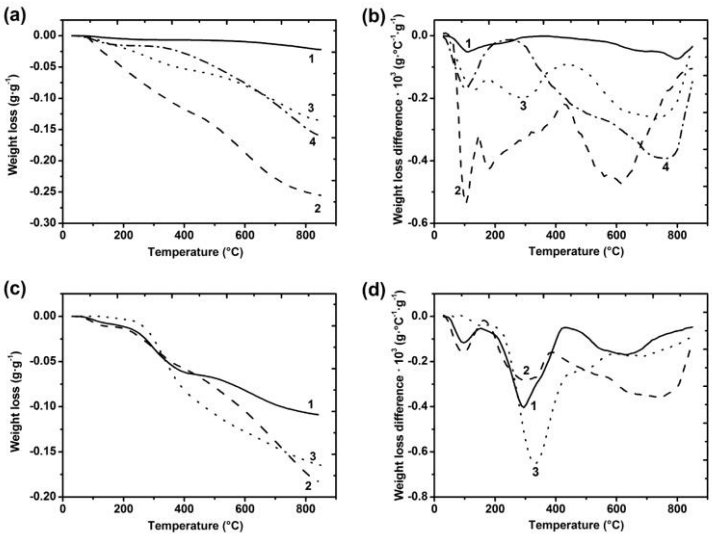

Fig. 3. TG (**a**, **c**) and DTG (**b**, **d**). **a**, **b**: SCN (**1**), SCNox (**2**), SCN-Br (**3**), and SCN-Cl (**4**); **c**, **d**: SCN-Br-N (**1**), SCN-Cl-N (**2**), and SCN-N (**3**).

Figure 3 imagines the results of the TG/DTG analysis of the SCN-based AC sorbents. The pristine SCN AC sorbent has a low content of surface oxygen-containing groups that correspond to a weight loss of 2.2%. The physisorbed water desorbs in the range 50–150 °C, while the thermal decomposition of the Ph groups takes place at 600–850 °C. Oxidation

of the SCN with HNO_3 is a reason for the formation of many different organic functional groups containing oxygen [18, 20]. For the sample of SCNox, the total weight loss increases by up to 25.5%. All Cx and a part of the A and L groups are decomposed between 170 and 450 °C. More thermostable A, L, and Ph groups are decomposed between 450 and 850 °C [21]. The bromination of the SCN AC sorbent increases the total weight loss effect by up to 13.5%. For the SCN-Br sample, in contrast with the pristine SCN sample, this weight loss is registered between 200 and 470 °C. It corresponds to the decomposition of a part of bromine-containing surface groups. At above 500 °C, the most stable forms of Br-containing and Ph groups, which formed because of the parallel oxidation of the surface by the action of KBr_3, are decomposed. For the SCN-Cl sample, besides water evaporation, the TG/DTG curves show a large weight loss above 350 °C. This effect includes the thermal decomposition of the Cl-containing and Ph groups between 600 and 850 °C. Unlike the sample of SCN-Br, only part (up to 40%) of chlorine can be removed from the surface of the SCN-Cl sample heated to 850 °C. The reactivity of chemisorbed bromine exceeds that of chlorine.

The intense effect of weight loss observed after the amination of the pristine and halogenated SCN samples. This effect is ranged from 200 to 450 °C (Figs. 3c and 3d) and has a peak temperature between 295 and 330 °C. We found the highest thermal stability of the amino groups in the SCN-N sample. Here, the amino groups showed a decomposition temperature of about 330 °C. At temperatures above 500 °C, the weight losses for the SCN-Br-N and SCN-N samples are similar. The grafted bromine is completely removed during the amination. Opposed to this observation, we registered a significant weight loss at high temperatures for the SCN-Cl-N sample. This weight loss corresponds to the removal of chlorine residues from this sorbent. Thus, the TG/DTG data show the high thermal stability of the aminated AC sorbents. Heating to 200 °C supports their fast dehydration and will ensure the complete removal of adsorbed CO_2 from the sorbents.

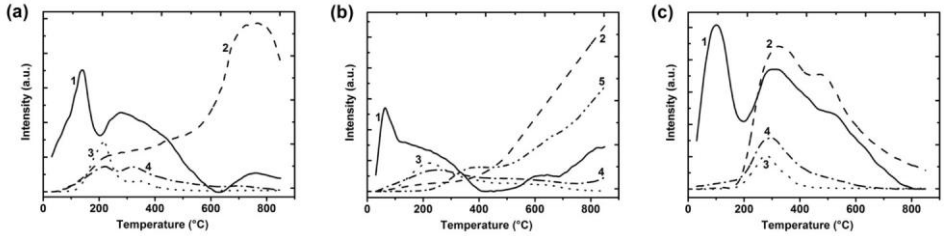

Fig. 4. Temperature-dependent mass selective ion current at m/z 18 (**1**), 28 (**2**), 30 (**3**), 44 (**4**), and 36 (**5**) in TPD MS analysis of SCN-Br-N (**a**), SCN-Cl-N (**b**), and SCN-N (**c**).

TPD MS confirms the results of TG/DTG analysis and shows the formation of $CH_2{=}N^+H_2$ ions (m/z 30), which are typical fragment ions [22] at the vacuum pyrolysis of the amino groups (Fig. 4). Profiles of $CH_2{=}N^+H_2$ have peaks at 205 °C (SCN-Br-N), 210 °C (SCN-Cl-N), and 265 °C (SCN-N). We associated high thermal stability of amino groups with other surface sites involved in the "direct" amination reaction, as compared with halogenation, followed by amination. Here, the decisive factor is the amination temperature of 230 °C. Thermal decomposition products of the aminated surface are also H_2O (m/z 18) and CO (m/z 28). The intensive MS signal of H_2O^+ between 200 and 400 °C is in a positive correlation with the MS signals of $CH_2{=}N^+H_2$ (m/z 30) and CO_2^+ (m/z 44). The latter signal is sourced from the products of vacuum pyrolysis of Cx groups and some A and L groups. Red-Ox transformations can also produce H_2O, CO, and CO_2 [23]. But, the main pyrolysis product at high temperatures is CO sourced from the Ph groups [24, 25]. A little part of the Ph groups is decomposed with the release of H_2O. That is why the data of the TPD MS and TG/DTG studies are in good agreement. It should be noticed that only a part of the chlorine

can be replaced by amino groups; see the MS signal of HCl (m/z 36) in Fig. 4b. HCl is a typical pyrolysis product when Cl-containing groups have decomposed in the presence of H-containing species.

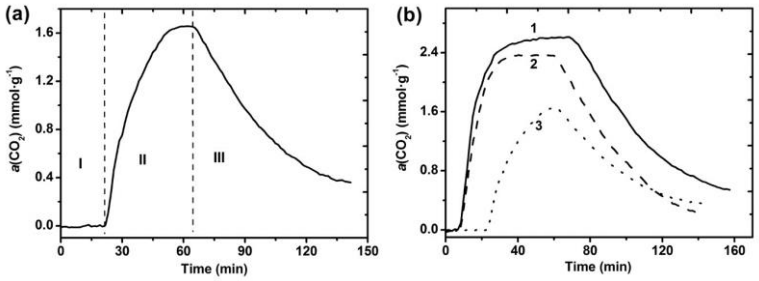

Fig. 5. Adsorption-desorption of CO_2 against time (**a**, **b**): ACB (**1**), SCN (**2**), and HSGD (**3**).

Disclosing adsorption-desorption behaviors, Fig. 5a shows three sections of the experimental curve registered by the thermogravimetric method. The first and second isothermal sections correspond to the argon purging and CO_2 adsorption up to a constant mass. The third section presents the thermodesorption of CO_2 registered from 20 to 100 °C under quasi-equilibrium conditions. Figure 5b shows that the sorbent regeneration is possible by heating the used sorbent above 100 °C. Both ACB and SCN sorbents have a high a_m of 2.4–2.6 mmol/g, while the HSGD sorbent shows a minimal a_m (Table 2).

Table 2. Functional groups concentration (C_{fg}) and CO_2 adsorption parameters.

Sorbent	*C_{fg}, mmol/g	Adsorption time, min		Adsorption capacity, mmol/g		
		τ(50%)	τ(90%)	a_m	a(50°C)	a(100°C)
ACB	0.88	7	19	2.61	1.61	0.35
SCN	0.93	9	19	2.39	1.24	0.25
HSGD	0.53	11	28	1.65	0.92	0.31

*C_{fg} is the concentration of O-containing groups

We assume the molecular packing of the adsorbed CO_2 within micropores. The adsorbed CO_2 should occupy 0.1 cm^3 per g, which is 20–25% of the numerical values of V_S for the pristine AC sorbents. We found no pronounced dependence of a_m on S_{BET} and V_S (cf. data in Tables 1 and 2). Of course, it is necessary to use materials having developed surface and porosity for adsorption of CO_2. But, it is impossible to predict the value of a_m in advance by considering texture only. Below we will disclose the impact of the functional groups on the adsorption of CO_2. Typical CO_2 adsorption/desorption curves are shown in Fig. 6.

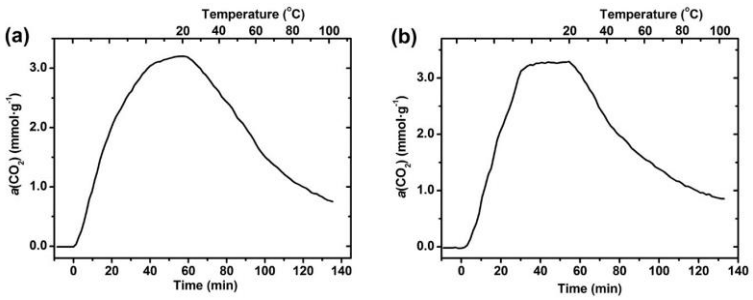

Fig. 6. Adsorption/desorption of CO_2 against time and temperature. (**a**) SCNox and (**b**) SCN-Br-N.

From the data comparison in Tables 2 and 3, one can see that the amination increases a_m by 30–55%. Despite the presence of many acidic surface groups, the values of a_m for the oxidized AC sorbents are higher than that of the pristine AC sorbents by 30–35%. This fact suggests that the oxygen-containing groups do not worsen but even improve the adsorption of CO_2.

Table 3. Functional groups concentration (C_{fg}) and CO_2 adsorption parameters.

Sorbent	C_{fg}, mmol/g	Adsorption time, min		Adsorption capacity, mmol/g		
		τ(50%)	τ(90%)	a_m	a(50°C)	a(100°C)
ACBox	5.49*	17	37	3.42	2.21	0.78
SCNox	5.28*	15	36	3.20	2.16	0.77
HSGDox	4.06*	16	38	2.22	1.43	0.41
ACB-Br-N	0.70**	18	29	3.51	1.95	0.89
SCN-Br-N	0.64**	17	28	3.29	1.87	0.86
HSGD-Br-N	0.59**	15	31	2.49	1.55	0.50
ACB-Cl-N	0.52**	14	23	3.32	1.92	0.96
SCN-Cl-N	0.51**	13	22	3.29	1.83	0.81
HSGD-Cl-N	0.47**	15	24	2.25	1.42	0.49
ACB-N	1.19**	12	23	3.89	2.39	1.07
SCN-N	1.06**	11	22	3.72	2.34	0.98
HSGD-N	0.85**	15	29	2.65	1.63	0.59

*C_{fg} is the concentration of O-containing groups; **C_{fg} is the concentration of amino groups.

One can explain the obtained results considering the high affinity of polar CO_2 molecules to polar surface groups. Liquid phase amination of pre-halogenated ACs can improve, to some extent, as compared with oxidation, the adsorption of CO_2. Comparing in pairs C_{fg} and a_m, one can see that the amino group is involved in the adsorption from 3 to 6 CO_2 molecules. Adsorbed CO_2 "islands" on the surface sections covered with amino groups can fulfill the required ratio. This is a rough approximation. However, the calculations confirm the positive impact of the carbon surface amination. Keeping in mind known amination methods [26], we showed that a positive effect on the adsorption of CO_2 is reached by a direct (gas-phase) introduction of diethylamino groups. Functionalization with basic diethylamino groups increases both τ(50%) and τ(90%) adsorption times to 11–18 and 22–38 minute periods, correspondingly. The aminated AC sorbents showed rapid saturation at the CO_2 adsorption. So, they will be effective in different applications. We described the thermal desorption of CO_2 from the sorbents saturated with CO_2 in the framework of the exponential model. According to our findings, the parameters a(50 °C) and a(100 °C) can reach values as high as 55–65% and 20–30% of a_m. This result proves that the aminated AC sorbents can uptake CO_2 at elevated temperatures. In contrast to the oxidized carbon surface, strong CO_2 adsorption on the aminated carbon surface limits the future regeneration of the AC sorbents.

4 Conclusions

According to the presented adsorption-desorption studies, functionalized ACs are effective sorbents for CO_2 capture from gas-phase. The structure parameters of the pristine AC sorbents are close. They don't have a decisive impact on CO_2 adsorption. Surface

functionalization with 0.47–1.2 mmol/g of diethylamino groups can increase the value of am up to 2.2–3.9 mmol of CO_2 per gram of sorbent. Oxidation of the AC sorbents can increase am by 25–30%, which is an important result. The presence of from 4.0 to 5.5 mmol of the surface O-containing groups per gram of sorbent can increase the CO_2 uptake up to 1.6–2.6 mmol/g. We showed that contrasting the pristine and oxidized ACs, the aminated ACs are characterized by a stronger bond between the surface sites and adsorbed CO_2.

V.V. Lisnyak is thankful to the International Visegrad Fund for the scholarship, ID number [51810574].

References

1. L. Cao, K. Caldeira, Environ. Res. Lett., **5**, 024011 (2010)
2. H. Tian, C. Lu, P. Ciais, A.M. Michalak, et al., Nature, **531**, 225 (2016)
3. T. Kuramochi, A. Ramírez, W. Turkenburg, et al. Prog. Energy. Combust. Sci., **38**, 87 (2012)
4. C.H. Yu, C.H. Huang, C.S. Tan, Aerosol Air Qual. Res., **12**, 745 (2012)
5. D.Y. Leung, G. Caramanna, M.M. Maroto-Valer, Renew. Sustain. Energy Rev., **39**, 426 (2014)
6. B.S. Caglayan, A.E. Aksoylu, J. Hazard. Mater., **252-253**, 19 (2013)
7. T.C. Drage, J.M. Blackman, C. Pevida, et al., Energy Fuels, **235**, 2790 (2009)
8. Y. Nakahigashi, H. Kanoh, T. Ohba, et al., Adsorpt. Sci. Technol., **30**, 621 (2012)
9. Y.C. Chiang, W.L. Hsu, S.Y. Lin, et al., Materials, **10**, 511 (2017)
10. D.P. Bezerra, F.W.M. da Silva, P.A.S. de Moura, et al., Adsorpt. Sci. Technol., **32**, 141 (2014)
11. W. Xie, M. Yu, R. Wang, Aerosol Air Qual. Res., **17**, 2715 (2017)
12. A. Houshmand, W.M.A.W. Daud, M.-G. Lee, et al., Water Air Soil Pollut., **223**, 827 (2012)
13. V.E. Diyuk, A.N. Zaderko, K.I. Veselovska, et al., J. Therm. Anal. Calorim., **120**, 1665 (2015)
14. V.E. Diyuk, R.T. Mariychuk, V.V. Lisnyak, J. Therm. Anal. Calorim., **124**, 119 (2016)
15. V.E. Diyuk, R.T. Mariychuk, V.V. Lisnyak, Mater. Chem. Phys., **184**, 138 (2016)
16. The Sadtler Handbook of Infrared Spectra (Bio-Rad Laboratories, Philadelphia, 2004)
17. L.M. Grishchenko, V.E. Diyuk, O.P. Konoplitska, et al., Adsorpt. Sci. Technol., **35**, 884 (2017)
18. J. Skubiszewska-Zięba, B. Charmas, M. Kołtowski, et al., J. Therm. Anal. Calorim., **130**, 15 (2017)
19. V.E. Diyuk, A.N. Zaderko, L.M. Grishchenko, et al., Catal. Commun., **27**, 33 (2012)
20. V.V. Multian, F.E. Kinzerskyi, A.V. Vakaliuk, et al., Nanoscale Res. Lett., **12**, 146 (2017)
21. W. Shen, Z. Li, Y. Liu, Rec. Pat. Chem. Enging. **1**, 27 (2008)
22. E.V. Basiuk, A. Santamaría-Bonfil, V. Meza-Laguna, et al., Appl. Surf. Sci., **275**, 324 (2013)
23. G. Hotová, V. Slovák, O.S.G.P. Soares, et al., Carbon, **134**, 255 (2018)
24. K.L. Klein, A.V. Melechko, T.E. McKnight, et al. J. Appl. Phys., **103**, 061301 (2008)
25. T. Ishii, T. Kyotani, Materials Science and Engineering of Carbon, edited by M. Inagaki (Elsevier, Amsterdam, 2016), pp. 287–305
26. M.S. Shafeeyan, W.M.A.W. Daud, A. Houshmand, et al., Appl. Surf. Sci., **257**, 3963 (2011)